Original Article

Multiparametric magnetic resonance imaging-based assessment of the effect of adenomyosis on determining the depth of myometrial invasion in endometrial cancer

Xuxu Meng[1#], Mingming Liu[2,3#], Dawei Yang[1], He Jin[1], Yun Liu[4], Hui Xu[1], Yuting Liang[2,3], Zhenchang Wang[1], Liang Wang[1], Zhenghan Yang[1]

[1]Department of Radiology, Beijing Friendship Hospital, Capital Medical University, Beijing, China; [2]Department of Radiology, Beijing Obstetrics and Gynecology Hospital, Capital Medical University, Beijing, China; [3]Department of Radiology, Beijing Maternal and Child Health Care Hospital, Beijing, China; [4]Department of Obstetrics and Gynecology, Beijing Friendship Hospital, Capital Medical University, Beijing, China

Contributions: (I) Conception and design: X Meng, D Yang, Y Liu, L Wang, Z Yang; (II) Administrative support: Z Yang; (III) Provision of study materials or patients: X Meng, L Wang, Z Yang; (IV) Collection and assembly of data: X Meng, M Liu; (V) Data analysis and interpretation: X Meng, M Liu, D Yang, H Jin; (VI) Manuscript writing: All authors; (VII) Final approval of manuscript: All authors.

[#]These authors contributed equally to this work.

Correspondence to: Zhenghan Yang, MD, PhD; Liang Wang, MD, PhD. Department of Radiology, Beijing Friendship Hospital, Capital Medical University, No. 95 Yong'an Road, Beijing, China. Email: yangzhenghan@vip.163.com; 1311935212@qq.com.

Background: Accurate preoperative diagnosis of endometrial cancer (EC) with deep myometrial invasion (DMI) is critical to deciding whether to perform lymphadenectomy. However, the presence of adenomyosis makes distinguishing DMI from superficial myometrial invasion (SMI) on magnetic resonance imaging (MRI) challenging. We aimed to evaluate the accuracy of multiparametric MRI (mpMRI) in diagnosing DMI in EC coexisting with adenomyosis (EC-A) compared with EC without coexisting adenomyosis and to evaluate the effect of different adenomyosis subtypes on myometrial invasion (MI) depth in EC.

Methods: Patients with histologically confirmed International Federation of Gynecology and Obstetrics (FIGO) stage I EC who underwent preoperative MRI were consecutively included in this 2-center retrospective study. Institution 1 was searched from January 2017 to November 2022 and institution 2 was searched from June 2017 to March 2021. Patients were divided into 2 groups: group A, patients with EC-A; group B, EC patients without coexisting adenomyosis, matched 1:2 according to age ±5 years and tumor grade. A senior radiologist assessed the MRI adenomyosis classification in group A. Then, 2 radiologists (R1/R2) independently interpreted T2-weighted imaging (T2WI), diffusion-weighted imaging (DWI), T1-weighted contrast-enhanced (T1CE), and a combination of all images (mpMRI) respectively, and then assessed MI depth. Accuracy, sensitivity, specificity, and the areas under the receiver operating curve (AUC) were calculated. The chi-square test was used to compare the accuracy of diagnosing DMI. Interobserver agreement was evaluated using the Kappa test.

Results: A total of 70 cases in group A and 140 cases in group B were included. The accuracy, sensitivity, and specificity of consensus were 94.3% [95% confidence interval (CI): 88.9–99.7%] *vs.* 92.1% (95% CI: 87.7–96.6%), 60.0% (95% CI: 17–92.7%) *vs.* 86.7% (95% CI: 68.4–95.6%), and 96.9% (95% CI: 88.4–95.5%) *vs.* 93.6% (95% CI: 86.8–97.2%) (group A *vs.* group B, respectively). There was no significant difference in the diagnostic accuracy of DMI on each sequence between the groups (Reviewer 1/Reviewer 2): P_{T2WI}=0.14/0.17, P_{DWI}=0.50/0.33, P_{T1CE}=0.90/0.18, P_{mpMRI}=0.50/0.37. The AUC for T2WI, DWI, T1CE, and mpMRI (Reviewer 1/Reviewer 2), respectively, were 0.54 (95% CI: 0.42–0.66)/0.78 (95% CI: 0.67–0.87), 0.63 (95% CI: 0.50–0.74)/0.77 (95% CI: 0.65–0.86), 0.69 (95% CI: 0.57–0.80)/0.79 (95% CI: 0.68–0.88), and 0.91 (95% CI: 0.82–0.97)/0.89 (95% CI: 0.79–0.95) (group A) and 0.83 (95% CI: 0.76–0.89)/0.85 (95%

CI: 0.78–0.90), 0.83 (95% CI: 0.76–0.89)/0.86 (95% CI: 0.79–0.91), 0.88 (95% CI: 0.82–0.93)/0.86 (95% CI: 0.80–0.92), and 0.91 (95% CI: 0.85–0.95)/0.87 (95% CI: 0.80–0.92) (group B). Interobserver agreement was highest with mpMRI [κ=0.387/0.695 (case/control)]. The consensus results of MRI categorization of adenomyosis revealed no significant difference in the accuracy of diagnosing DMI by adenomyosis subtype ($P_{spatial\ relationship}$>0.99, $P_{affected\ area}$=0.52, $P_{affected\ pattern}$=0.58, $P_{affected\ size}$>0.99).

Conclusions: The presence of adenomyosis or adenomyosis subtype had no significant effect on the interpretation of the depth of MI. T1CE can increase the contrast between adenomyosis and cancer foci; therefore, the information provided by T1CE should be valued.

Keywords: Endometrial cancer (EC); adenomyosis; deep myometrial invasion (DMI); magnetic resonance imaging (MRI)

Submitted Nov 15, 2023. Accepted for publication Mar 20, 2024. Published online Apr 26, 2024.
doi: 10.21037/qims-23-1621
View this article at: https://dx.doi.org/10.21037/qims-23-1621

Introduction

Endometrial cancer (EC) is a common malignant reproductive system tumor in women, which has recently exhibited a gradual increase in incidence and mortality. According to the Global Cancer Statistics Report, 413,367 new cases of EC (approximately 2.2% of all cancers) and 97,370 new deaths were reported worldwide in 2020 (1). Hysterectomy with bilateral salpingo-oophorectomy, with or without removal of the pelvic and para-aortic lymph nodes, is currently a radical treatment for patients with EC. Preoperative magnetic resonance imaging (MRI) staging is useful to develop a personalized treatment plan (2,3). The depth of myometrial invasion (MI) in EC is considered an important factor closely related to lymph node metastasis and prognosis. A previous study (4) reported a much higher rate of lymph node metastasis in stage I EC with deep myometrial invasion (DMI) compared with superficial myometrial invasion (SMI) (46% *vs.* 3%, respectively). There is still controversy as to whether patients with SMI need to undergo lymphadenectomy, but patients with DMI are usually recommended to undergo lymphadenectomy or sentinel lymph node biopsy (5). In addition, adjuvant treatment options vary among patients with different depths of MI or risk stratification. The European Society of Gynecological Oncology-European Society for Radiotherapy and Oncology-European Society for Pathology (ESGO-ESTRO-ESP) guidelines (6) state that adjuvant therapy is not recommended for low-risk ECs [stage 1A, endometrioid, low grade, lymph vascular space invasion (LVSI) negative or focal]. For patients at intermediate (e.g., stage 1B endometrioid, low-grade, LVSI negative or focal) or higher risk, adjuvant therapy is recommended. Therefore, accurate preoperative assessment of the depth of MI is essential for prognosis and adjuvant therapy options in patients with EC.

MRI and transvaginal ultrasound are the main methods to evaluate the depth of MI preoperatively (7). Preoperative MRI is the first choice to determine the International Federation of Gynecology and Obstetrics (FIGO) stage of EC and has high sensitivity and specificity for the detection of DMI (8). Several meta-analyses (9-11) have reported that the sensitivity and specificity of MRI for assessing DMI range from 0.77 to 0.86 and 0.81 to 0.88, respectively. However, several studies (12-15) have reported several confounding factors in the interpretation of the depth of MI, namely adenomyosis, tumor extension to the uterine cornu, and the presence of leiomyomas. Notably, adenomyosis has been identified in 9–34% of resected specimens from patients with EC (16,17). A meta-analysis showed an overall prevalence of adenomyosis in EC patients of 22.6% (18). These findings suggest that EC coexisting with adenomyosis (EC-A) is not uncommon. However, the presence of adenomyosis makes it challenging to evaluate MI with imaging, especially for ultrasound. In 2004, Utsunomiya *et al.* (19) used T2-weighted imaging (T2WI) and dynamic T1-weighted imaging (T1WI) with contrast enhancement to assess the depth of MI in 12 lesions of EC-A. The results showed that 7 lesions were misinterpreted or undetectable on T2WI, and 2 lesions were misinterpreted on dynamic T1WI. However, the study focused only on 2 sequences of T2WI and T1-weighted contrast-enhanced (T1CE) imaging and did not evaluate the role of multiparametric MRI (mpMRI) in interpreting images.

Subsequent studies (12,13,20) have shown that EC-A can lead to varying degrees of misinterpretation of the depth of MI. Rockall *et al.* (13) reported a misjudgment rate of 10% (1/10), and the misjudgment rate of Sala *et al.* (20) was 16.7% (1/6). Although these studies indicated that EC with or without coexisting adenomyosis was not associated with incorrect assessment of the depth of MI, the small sample sizes in these studies did not allow for an accurate assessment of the true impact of adenomyosis on MI in EC. Additionally, adenomyosis shows variable findings on imaging, and several MRI classifications of adenomyosis have been proposed (21-25). The impact of different adenomyosis subtypes on the assessment of the depth of MI in EC also is unknown. Therefore, the objectives of the present study were as follows: the primary objective was to evaluate the accuracy of mpMRI in the diagnosis of DMI in group A (EC-A) compared with group B (EC without coexisting adenomyosis) by sufficient sample size; the second objective was to evaluate the effect of different subtypes of adenomyosis in the interpretation of MI in EC. In this study, mpMRI was defined as a combination of multiple sequences including T1WI, T2WI, diffusion-weighted imaging (DWI) with apparent diffusion coefficient (ADC), and T1CE. We present this article in accordance with the STARD reporting checklist (available at https://qims.amegroups.com/article/view/10.21037/qims-23-1621/rc).

Methods

Medical records with postoperative pathology confirming EC were consecutively searched from the Beijing Friendship Hospital Affiliated to Capital Medical University (institution 1) and Beijing Obstetrics and Gynecology Hospital Affiliated to Capital Medical University (institution 2) respectively, with institution 1 searched from January 2017 to November 2022 and institution 2 searched from June 2017 to March 2021.

This study was a case-control retrospective trial. The inclusion criteria for group A were as follows: (I) EC confirmed by pathology; (II) adenomyosis also confirmed by pathology; (III) preoperative contrast-enhanced MRI of the pelvis; (IV) EC lesions visible on imaging; and (V) time interval from MRI to surgery <60 days. The exclusion criteria were as follows: (I) non-stage 1 EC (26); (II) presence of other pelvic malignancies (e.g., ovarian cancer); (III) multiple fibroids that affected the interpretation of the depth of MI; (IV) history of preoperative neoadjuvant therapy; and (V) poor image quality or incomplete images. Group B comprised patients with stage I EC without coexisting adenomyosis, matched 2:1 by age (±5 years) and tumor grade with a patient in group A. The inclusion and exclusion criteria for group B were the same as those for group A, except for the absence of adenomyosis.

The study was conducted in accordance with the Declaration of Helsinki (as revised in 2013). The study was approved by institutional ethics boards of Beijing Friendship Hospital Affiliated to Capital Medical University (No. YYXSSC-2022-073) and Beijing Obstetrics and Gynecology Hospital Affiliated to Capital Medical University (No. 2022-KY-061-01), and the requirement for individual consent for this analysis was waived due to the retrospective nature.

Imaging acquisition

All MRI examinations were obtained using 1.5- or 3.0-T scanners using a pelvic phased-array surface coil. Each patient fasted for 6 hours prior to the examination. Patients were placed in the supine position, and the center of localization was 2 cm above the midpoint of the pubic symphysis. The scanning range encompassed the uterus and bilateral appendages. Non-contrast enhanced scans comprised T2WI, T1WI, and DWI (b=0 and b=800/1,000 s/mm^2). T1CE was also performed, after injection of gadopentetate dimeglumine at a dose of 0.1 mmol/kg. Fat-suppressed T1WI was acquired in the axial, sagittal, and coronal planes (before, 30, 70, and 240 s after contrast injection in the sagittal plane; 150 s after contrast injection in the axial oblique plane; and 300 s after contrast injection in the coronal plane). The MRI protocol parameters are shown in Tables S1-S4.

Imaging analysis

All MR images were imported into a Picture Archiving and Communication System (PACS; DJ Health Union Systems Corp., Shanghai, China). First, the classification of adenomyosis in group A was performed by a senior radiologist (with 18 years of experience in gynecological imaging). At present, there is no consensus on the MRI classification of adenomyosis. In order to facilitate radiologists to perform MRI classification of adenomyosis, we chose the Kobayashi classification (23) as the standard for this study. The classifications were as follows:

- Spatial relationship: adenomyotic lesions and cancer foci in close proximity were defined as

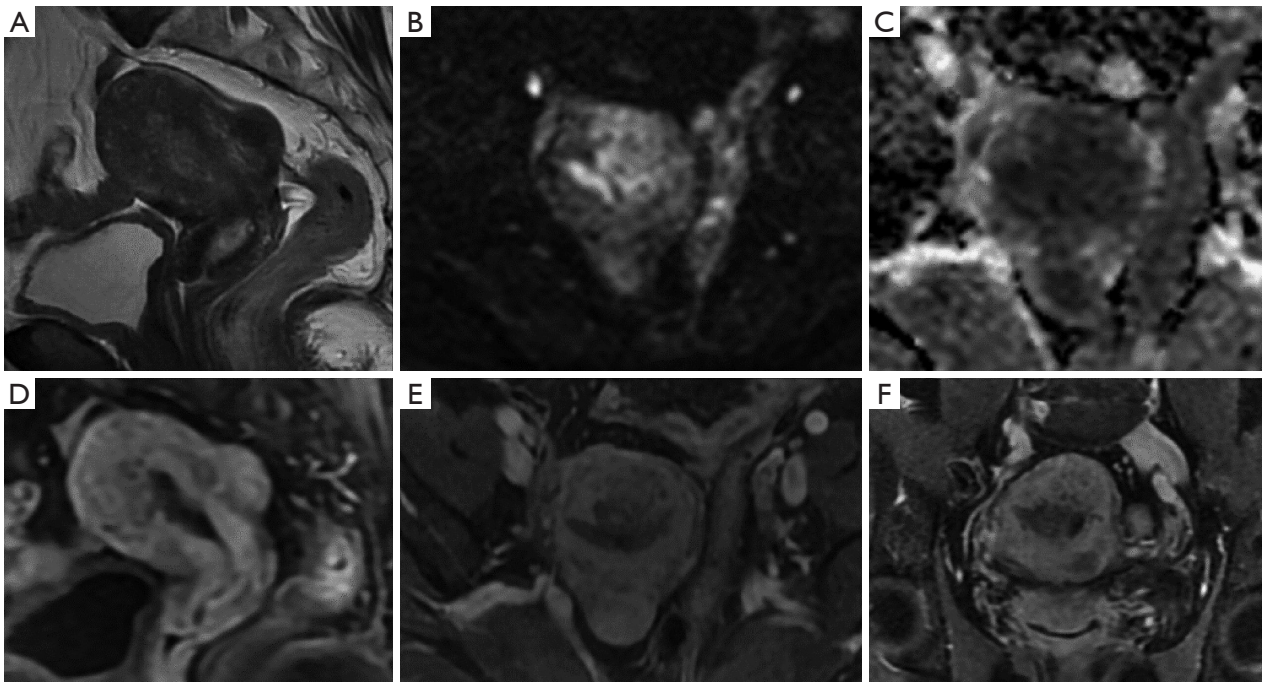

Figure 1 A 61-year-old patient with an endometrioid cancer (G1) coexisting adenomyosis and surgical pathology confirmed FIGO stage IA. (A) sagittal oblique T2WI, (B) axial diffusion weighted (b=1,000 s/mm^2), (C) axial apparent coefficient diffusion map, (D) sagittal delayed-phase T1CE scan 150 s after gadolinium chelate injection, (E) axial oblique delayed-phase T1CE scan 180 s after gadolinium chelate injection, and (F) coronal delayed-phase T1CE scan 240 s after gadolinium chelate injection. The spatial relationship between the adenomyotic lesion and the cancer foci is adjacent. Diffuse adenomyosis is poorly demarcated from endometrial cancer, which is difficult to diagnose the depth of myometrial invasion on T2WI and DWI. T1CE increases the contrast between the lesions. Signal differences between endometrial cancer and adenomyosis at the continuation should be carefully discerned on T1CE. G, grade; FIGO, International Federation of Gynecology and Obstetrics; T2WI, T2-weighted imaging; DWI, diffusion-weighted imaging; T1CE, T1-weighted contrast-enhanced.

adjacent (*Figure 1*) and vice versa as non-adjacent (*Figure 2*).

- Affected area: an affected area within the inner 1/3 of the uterine wall was defined as internal adenomyosis. An affected area within the outer 2/3 of the myometrium was defined as external adenomyosis.
- Affected pattern: the affected pattern was classified as diffuse or focal.
- Affected size: the affected size was divided into thirds: <1/3, <2/3, or >2/3 of the uterine wall.

The depth of MI on MR images was independently interpreted by 2 radiologists (radiologist 1 X.M. and radiologist 2 H.J.) with 4 and 10 years of gynecological imaging experience, respectively. Both radiologists were unaware of the depth of MI pathologically, and the radiologists who reviewed the images was not involved initially in the cases. The image analysis was performed in multiple rounds, and the order of the images in each round was randomized. T2WI, DWI with ADC, T1CE, and mpMRI were interpreted in turn. The mpMRI readings simulated interpretation in clinical practice, mainly including T1WI, T2WI, DWI with ADC, and T1CE. The time interval between each round of reading was 3 weeks. When mpMRI-based results were inconsistent, a third round of image reading was performed by a senior radiologist (D.Y.) with 18 years of experience in gynecological imaging, to reach consensus.

MRI interpretation criteria for MI depth

MI appeared as an interrupted or irregular junctional zone of low signal on T2WI and interrupted rings of subendometrial enhancement on T1CE. Tumor invasion

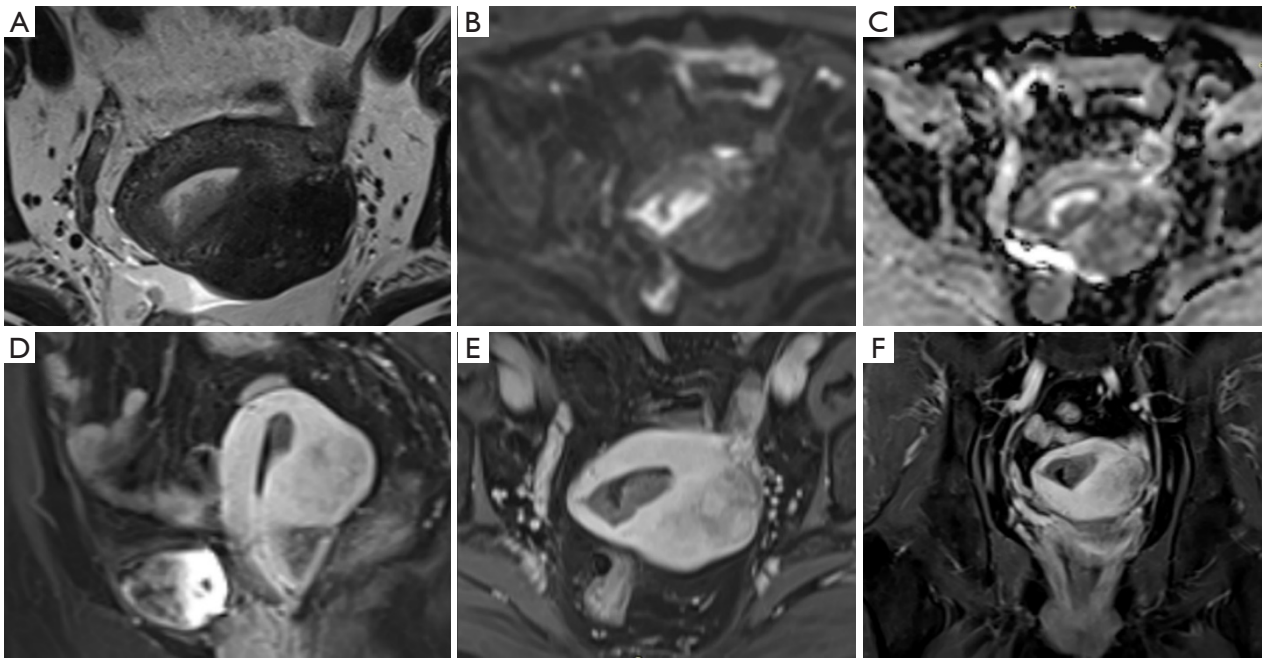

Figure 2 A 60-year-old patient with an endometrioid cancer (G1) coexisting adenomyosis and surgical pathology confirmed FIGO stage IA. (A) axial oblique T2WI, (B) axial diffusion weighted (b=1,000 s/mm^2), (C) axial apparent coefficient diffusion map, (D) sagittal delayed-phase T1CE MRI scan 150 s after gadolinium chelate injection, (E) axial oblique delayed-phase T1CE scan 180 s after gadolinium chelate injection, and (F) coronal delayed-phase T1CE scan 240 s after gadolinium chelate injection. Adenomyosis was located in the outer myometrium of the corpus uteri and is not adjacent to endometrial cancer foci. And adenomyosis did not affect the identification of the depth of myometrial infiltration in this case. G, grade; FIGO, International Federation of Gynecology and Obstetrics; T2WI, T2-weighted imaging; T1CE, T1-weighted contrast-enhanced; MRI, magnetic resonance imaging.

exceeding 1/2 of the myometrium was defined as DMI, otherwise it is defined as SMI. The depth of MI was assessed visually using 2 scoring systems. System 1 was a dichotomous system. An MI depth was recorded as DMI or SMI. System 2 was a 5-point system (1: positive SMI; 2: possible SMI; 3: uncertain; 4: possible DMI; 5: positive DMI). Using these scoring systems, the radiologists were asked to record the readings in sequence in a preset Excel (Microsoft Inc., Redmond, WA, USA) form.

Histopathological analysis

All recruited patients underwent hysterectomy with bilateral salpingo-oophorectomy at both institutions. After specimen processing, samples were collected by a gynecological pathologist. Two gynecological pathologists (all with >5 years of experience in gynecologic pathology) then analyzed the findings and confirmed the presence of adenomyosis in each institution. Tumor tissue infiltration exceeding 1/2 of the muscle layer depth was defined as DMI (27). The histopathology report was reviewed by a radiologist, and the depth of the MI was documented.

Sample size calculation and statistical analysis

A formal statistical power analysis was used to determine the minimum acceptable sample size. On the basis of our pre-experimental results (odds ratio =0.32, P0=0.30) and assuming α=0.05 and a case: control ratio of 1:2, we calculated the sample size required for 80% power (PASS, version 2020; https://www.ncss.com/software/pass/). The results of the power analysis indicated that a minimum of 64 patients were required to reach 80% power in group A.

The chi-square test was used to compare the differences in interpretation results (correct or incorrect) between group A and B and between different subtypes of adenomyosis. All statistical analyses were performed using SPSS 25.0 (IBM Corp., Armonk, NY, USA). The sensitivity, specificity, positive predictive value (PPV), negative predictive value (NPV), and accuracy were calculated to

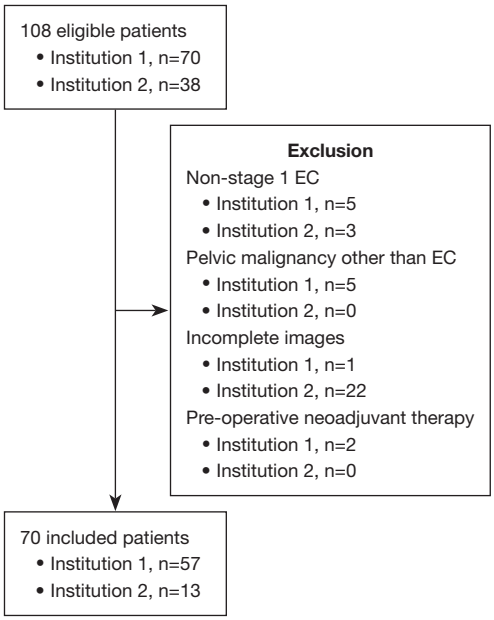

Figure 3 Flowchart of patient selection for group A at the two recruiting institutions. Group A, endometrial cancer coexisting with adenomyosis. Institution 1: Beijing Friendship Hospital Affiliated to Capital Medical University; institution 2: Beijing Obstetrics and Gynecology hospital Affiliated to Capital Medical University. EC, endometrial cancer.

evaluate the performance of MRI in diagnosing DMI by the dichotomous system. The areas under the receiver operating characteristic (ROC) curve (AUC) were also assessed by the 5-point system. MedCalc 20 (MedCalc Software, Mariakerke, Belgium) was used to compare differences between the case and control groups. Interobserver agreement was assessed using Kappa test and interpreted as follows: poor (0.20), fair (0.20–0.39), moderate (0.40–0.59), good (0.60–0.79), or excellent (0.80–1.00). A P value <0.05 was considered a significant difference by 2-sided test.

Results

Patient characteristics

A total of 70 patients with EC-A were included in this study (*Figure 3*): 57 from institution 1 and 13 from institution 2. A total of 140 controls were included in this study, all from institution 1. The patients' characteristics are shown in *Table 1*, which shows that the pathological type was endometrioid carcinoma in all patients in both groups. The average age was 54.20±8.20 and 55.71±8.26 years in group A and B, respectively, with no significant difference between the groups (P=0.21). There were 5 (7.1%) and 30 (21.4%) cases of DMI in group A and B, respectively.

Table 1 Patient characteristics.

Characteristics	Group A (n=70)	Group B (n=140)	P value
Age(year), mean ± SD	54.20±8.20	55.71±8.26	0.21
Pathological type, n (%)			–
Endometrioid carcinoma	70 (100)	140 (100)	
Non-endometrioid carcinoma	0 (0)	0 (0)	
Tumor grade, n (%)			>0.99
Low grade	67 (95.7)	134 (95.7)	
High grade	3 (4.3)	6 (4.3)	
Myometrial invasion, n (%)			0.01
DMI	5 (7.1)	30 (21.4)	
SMI	65 (92.9)	110 (78.6)	
Field strength, n (%)			0.09
1.5T	9 (12.9)	32 (22.9)	
3.0T	61 (87.1)	108 (77.1)	

Group A, patients with endometrial cancer coexisting with adenomyosis; Group B, patients with endometrial cancer without coexisting with adenomyosis. SD, standard deviation; DMI, deep myometrial invasion; SMI, superficial myometrial invasion.

Table 2 Results of 2 reviewers for identifying the depth of MI correct or incorrect on each sequence

Reviewer and modality	T2WI			DWI			T1CE			mpMRI		
	Cases	Controls	P value	Cases	Controls	P value	Cases	Controls	P value	Cases	Controls	P value
Reviewer 1			0.14			0.50			0.90			0.51
Undervalued	3 (4.3)	7 (5.0)		1 (1.4)	6 (4.3)		1 (1.4)	2 (1.4)		1 (1.4)	3 (2.1)	
Correct	49 (70.0)	111 (79.3)		50 (71.4)	106 (75.7)		58 (82.9)	117 (83.6)		62 (88.6)	128 (91.4)	
Overvalued	18 (25.7)	22 (15.7)		19 (27.1)	28 (20.0)		11 (15.7)	21 (15.0)		7 (10.0)	9 (6.4)	
Reviewer 2			0.17			0.33			0.18			0.37
Undervalued	3 (4.3)	9 (6.4)		2 (2.9)	7 (5.0)		3 (4.3)	8 (5.7)		3 (4.3)	8 (5.7)	
Correct	65 (92.9)	121 (86.4)		65 (92.9)	124 (88.6)		66 (94.3)	124 (88.6)		66 (94.3)	127 (87.9)	
Overvalued	2 (2.9)	10 (7.1)		3 (4.3)	9 (6.4)		1 (1.4)	8 (5.7)		1 (1.4)	5 (3.6)	

Data are presented as n (%). Cases, patients with endometrial cancer coexisting with adenomyosis (group A); controls, patients with endometrial cancer without coexisting with adenomyosis (group B). MI, myometrial invasion; T2WI, T2-weighted imaging; DWI, diffusion-weighted imaging; T1CE, T1-weighted contrast-enhanced; mpMRI, multiparametric magnetic resonance imaging.

Misinterpretation rate of DMI (group A vs. group B)

From *Table 2*, the error rates (Reviewer 1/Reviewer 2) in identifying DMI using T2WI, DWI, T1CE, and mpMRI were 30.0%/7.2%, 28.6%/7.2%, 17.1%/5.7%, and 11.4%/5.7% in group A, and 20.7%/13.5%, 24.3%/11.4%, 16.4%/11.4%, and 8.5%/9.3% in group B, respectively. There were no significant differences (R1/R2) in misinterpreting DMI between the groups: P_{T2WI}=0.14/0.17, P_{DWI}=0.50/0.33, P_{T1CE}=0.90/0.18, and P_{mpMRI}=0.51/0.37.

Diagnostic performance of MRI in 2 groups

For Reviewer 1, in group A, T2WI had the lowest sensitivity (40.0%), and DWI had the lowest specificity (70.8%). Similarly, in group B, T2WI had the lowest sensitivity (76.7%), and DWI the lowest specificity (74.5%). Reviewer 2, as a senior and experienced gynecological radiologist, had very similar accuracy in identifying DMI on each sequence. The consensus results were as follows: the sensitivity of MRI in group A was 60.0%, and the specificity was 96.9%. The sensitivity of MRI in group B was 86.7%, and the specificity was 93.6%. There was no significant difference in accuracy between the groups (*Tables 3*,*4*). Furthermore, we conducted a chi-square test on the misjudgments of DMI or SMI between the 2 groups, and the results are presented in *Table 5*. In group A, 2 out of 5 DMI cases were underestimated, whereas in group B, only 4 out of 30 DMI cases were underestimated.

We further analyzed the ROCs for identifying DMI, and the results are shown in *Table 6*. For Reviewer 1, the AUCs of T2WI, DWI, T1CE, and mpMRI for identifying DMI increased progressively in group A, with the lowest AUC of 0.54 for T2WI and the highest AUC of 0.91 for mpMRI. The AUCs of T2WI, DWI, and T1CE in group B were higher than those in group A for Reviewer 1, and the AUCs of mpMRI were similar in 2 groups. For Reviewer 2, the AUC was highest for mpMRI at 0.89, and the remaining 3 sequences had similar AUCs (0.78–0.79) in group A. The AUC values were very close between the sequences in group B. Independent ROC curve comparison analysis showed significant differences in AUCs between 2 groups with T2WI for Reviewer 1 (P=0.04). There were no significant differences in AUCs between group A and B for DWI, T1CE, and mpMRI (Figure S1).

Interobserver agreement

We calculated the concordance between the 2 reviewers for detecting DMI in both groups (*Table 7*). Generally, the highest concordance was found in both group A and group B for mpMRI ($\kappa_{case\ group}$=0.387, $\kappa_{control\ group}$=0.695). Group A and group B had the lowest concordance for DWI, with κ values of 0.242 and 0.535, respectively. The concordance of each sequence in group B was higher than that of the corresponding sequence in group A.

Diagnostic performance of MRI with different classifications of adenomyosis

As adenomyosis could not be visualized on MRI in

Table 3 Diagnostic performance of two reviewers for DMI identification

Reviewer and modality	T2WI		DWI		T1CE		mpMRI	
	Cases	Controls	Cases	Controls	Cases	Controls	Cases	Controls
Reviewer 1, % (95% CI)								
Accuracy	70.0 (59.3–80.7)	79.3 (72.6–86.0)	71.4 (60.9–82.0)	75.7 (68.6–82.8)	82.9 (74.0–91.7)	83.6 (77.4–89.7)	88.6 (81.1–96.0)	91.4 (86.8–96.1)
Sensitivity	40.0 (7.3–83.0)	76.7 (57.3–89.4)	80.0 (29.9–98.9)	80.0 (60.9–91.6)	80.0 (29.9–98.9)	93.3 (76.5–98.8)	80.0 (29.9–98.9)	90.0 (72.3–97.4)
Specificity	72.3 (59.6–82.3)	80.0 (71.1–86.8)	70.8 (58.0–81.1)	74.5 (65.2–82.2)	83.1 (71.3–90.9)	80.9 (72.1–87.5)	89.2 (78.5–95.2)	84.2 (76.1–90.0)
NPV	94.0 (82.5–98.4)	92.6 (84.9–96.7)	97.9 (87.3–99.9)	93.2 (85.2–97.2)	98.2 (89.0–99.9)	97.8 (91.5–99.6)	98.3 (89.7–99.9)	97.1 (91.2–99.3)
PPV	10.0 (1.8–33.1)	51.1 (36.0–66.1)	17.4 (5.7–39.5)	46.2 (32.5–60.0)	26.7 (8.9–55.2)	57.1 (42.3–70.9)	36.4 (12.4–68.4)	58.7 (43.3–72.7)
Reviewer 2, % (95% CI)								
Accuracy	92.9 (86.8–98.9)	86.4 (80.8–92.1)	92.9 (86.8–98.9)	88.6 (83.3–93.8)	94.3 (88.9–99.7)	88.6 (83.3–93.8)	94.3 (88.9–99.7)	90.7 (85.9–95.5)
Sensitivity	40.0 (7.3–83.0)	70.0 (50.4–84.6)	60.0 (17.0–92.7)	76.7 (57.3–89.4)	40.0 (7.3–83.0)	73.3 (53.8–87.0)	40.0 (7.3–83.0)	73.3 (53.3–87.0)
Specificity	96.9 (88.4–99.5)	90.9 (83.5–95.3)	95.4 (86.2–98.8)	91.8 (84.6–96.0)	98.4 (90.6–99.9)	92.7 (85.7–96.6)	98.4 (90.6–99.9)	95.5 (89.2–98.3)
NPV	95.5 (86.4–98.8)	91.7 (84.5–95.9)	96.9 (88.1–99.5)	93.5 (86.6–97.1)	95.5 (86.6–98.8)	92.7 (85.7–96.6)	95.5 (86.6–98.8)	92.9 (86.1–96.7)
PPV	50.0 (9.2–90.8)	67.7 (48.5–82.7)	50.0 (13.9–86.1)	71.9 (53.0–85.6)	66.7 (12.5–98.2)	73.3 (53.8–87.0)	66.7 (12.5–98.2)	81.5 (61.3–93.0)

Cases, patients with endometrial cancer coexisting with adenomyosis (group A); controls, patients with endometrial cancer without coexisting with adenomyosis (group B). DMI, deep myometrial invasion; T2WI, T2-weighted imaging; DWI, diffusion-weighted imaging; T1CE, T1-weighted contrast-enhanced; mpMRI, multiparametric magnetic resonance imaging; CI, confidence interval; NPV, negative predictive value; PPV, positive predictive value.

Table 4 Diagnostic efficacy of to identify DMI after consensus

Group	Accuracy, % (95% CI)	Sensitivity, % (95% CI)	Specificity, % (95% CI)	NPV, % (95% CI)	PPV, % (95% CI)	P
Group A	94.3 (88.9–99.7)	60.0 (17.0–92.7)	96.9 (88.4–95.5)	60.0 (17.0–92.7)	96.9 (88.3–99.5)	0.57
Group B	92.1 (87.7–96.6)	86.7 (68.4–95.6)	93.6 (86.8–97.2)	96.3 (90.1–98.8)	78.8 (60.6–90.4)	

Group A, patients with endometrial cancer coexisting with adenomyosis; Group B, patients with endometrial cancer without coexisting with adenomyosis. DMI, deep myometrial invasion; CI, confidence interval; NPV, negative predictive value; PPV, positive predictive value.

2 patients, 68 patients were included in the analysis of adenomyosis subtypes. Generally, EC coexisting with different classifications of adenomyosis (adjacent *vs.* non-adjacent, internal *vs.* external, diffuse *vs.* focal, <1/3 of the uterine wall *vs.* <2/3 of the uterine wall *vs.* >2/3 of the uterine wall) showed no significant difference in accuracy for identifying DMI (*Table 8*). As shown in Table S5, Reviewer 1 was significantly more accurate in identifying DMI with diffuse adenomyosis compared with focal adenomyosis on T2WI (P=0.03); significantly more accurate in the subgroup with adenomyosis involving <1/3 of the uterine wall compared with the other 2 subgroups on T2WI (P=0.04); and significantly more accurate with internal adenomyosis compared with external adenomyosis on

Table 5 AUC values acquired based on MRI for identifying DMI of two reviewers

Reviewer and modality	T2WI			DWI			T1CE			mpMRI		
	Cases	Controls	P value	Cases	Controls	P value	Cases	Controls	P value	Cases	Controls	P value
Reviewer 1			0.04			0.16			0.18			0.99
AUC (95% CI)	0.54 (0.42–0.66)	0.83 (0.76–0.89)		0.63 (0.50–0.74)	0.83 (0.76–0.89)		0.69 (0.57–0.80)	0.88 (0.82–0.93)		0.91 (0.82–0.97)	0.91 (0.85–0.95)	
Reviewer 2			0.61			0.49			0.57			0.90
AUC (95% CI)	0.78 (0.67–0.87)	0.85 (0.78–0.90)		0.77 (0.65–0.86)	0.86 (0.79–0.91)		0.79 (0.68–0.88)	0.86 (0.80–0.92)		0.89 (0.79–0.95)	0.87 (0.80–0.92)	

Cases, patients with endometrial cancer coexisting with adenomyosis (group A); controls, patients with endometrial cancer without coexisting with adenomyosis (group B). AUC, area under the curve; MRI, magnetic resonance imaging; DMI, deep myometrial invasion; T2WI, T2-weighted imaging; DWI, diffusion-weighted imaging; T1CE, T1-weighted contrast-enhanced; mpMRI, multiparametric magnetic resonance imaging; CI, confidence interval.

Table 6 Inter-observer agreement analysis for each sequence

Group	Sequence	Concordant, n (%)	Discordant, n (%)	Kappa
Group A	T2WI	54 (77.1)	16 (22.9)	0.263
	DWI	51 (72.9)	19 (27.1)	0.242
	T1CE	58 (82.9)	12 (17.1)	0.282
	mpMRI	62 (88.6)	8 (11.4)	0.387
Group B	T2WI	114 (81.4)	26 (18.6)	0.536
	DWI	112 (80.0)	28 (20.0)	0.535
	T1CE	121 (86.4)	19 (13.6)	0.672
	mpMRI	125 (89.3)	15 (10.7)	0.695

Group A, patients with endometrial cancer coexisting with adenomyosis; Group B, patients with endometrial cancer without coexisting with adenomyosis. T2WI, T2-weighted imaging; DWI, diffusion-weighted imaging; T1CE, T1-weighted contrast-enhanced; mpMRI, multiparametric magnetic resonance imaging.

Table 7 Diagnostic performance based on consensus of different subtypes of adenomyosis for DMI identification

Subtype	Classification	Accuracy (%)	Sensitivity (%)	Specificity (%)	NPV (%)	PPV (%)
Spatial	Adjacent	93.1	66.7	96.2	96.2	66.7
Relationship	Non-adjacent	94.9	50.0	97.3	97.3	50.0
Affected area	Internal adenomyosis	94.7	50.0	98.1	96.3	66.7
	External adenomyosis	90.9	100.0	90.0	100.0	50.0
Affected pattern	Diffuse	95.7	50.0	97.8	97.8	50.0
	Focal	90.5	66.7	94.4	94.4	66.7
Affected size	<1/3 of uterine wall	91.7	50.0	100.0	90.0	100.0
	<2/3 of uterine wall	95.8	100.0	95.5	100.0	66.7
	>2/3 of uterine wall	93.8	0.0	96.8	96.8	0.0

DMI, deep myometrial invasion; NPV, negative predictive value; PPV, positive predictive value.

Table 8 A 2×2 table for mpMRI diagnosis of MI depth after consensus

Group	DMI			SMI		
	Correct	Incorrect	P value	Correct	Incorrect	P value
Group A	3	2	0.20	63	2	>0.99
Group B	26	4		107	3	

Group A, patients with endometrial cancer coexisting with adenomyosis; Group B, patients with endometrial cancer without coexisting with adenomyosis. mpMRI, multiparametric magnetic resonance imaging; MI, myometrial invasion; DMI, deep myometrial invasion; SMI, superficial myometrial invasion.

T1CE (P=0.01). In contrast, for Reviewer 2, there was no statistical difference in accuracy for detecting DMI between the different categories of adenomyosis with coexisting EC. As demonstrated in *Table 8*, all subtypes of adenomyosis coexisting with EC were associated with excellent accuracy for MRI in detecting DMI.

Discussion

The aim of this study was to evaluate the accuracy of mpMRI in diagnosing DMI. Previously, several authors (19,28,29) have investigated the confounding factors for preoperative MRI assessment of the depth of MI in EC. Some studies (19,28,29) compared the accuracy of the depth of MI between different sequences, such as T2WI versus T1CE. Other studies (12-14) have identified multiple factors associated with misjudging the depth of MI, namely uterine fibroids, absence of the uterine junctional zone, and polypoid tumors. Unlike previous studies, the present study evaluated the effect of adenomyosis (including different classifications of adenomyosis) on the interpretation of the depth of MI (SMI or DMI) in EC using preoperative MRI. Through a formal statistical power analysis, our study included a sufficient sample size. Our results are similar to those of previous small sample studies: there was no significant effect of the presence of adenomyosis on the accuracy of detecting DMI (P>0.05). Furthermore, our results also show that there was no significant effect of the presence of different subtypes of adenomyosis (adjacent *vs.* non-adjacent, internal *vs.* external, diffuse *vs.* focal, <1/3 of the uterine wall *vs.* <2/3 of the uterine wall *vs.* >2/3 of the uterine wall) on the accuracy of detecting DMI (P>0.05).

The final misinterpretation rate of group A in this study was 5.7% (4/70), similar to the results of previous studies (12,13,20). The results of Reviewer 1 showed that most of the misclassified cases were overestimated DMI. Although we found no similar reports, we speculate that this result was associated with a lack of clinical experience and concern about missing cases. Unlike Reviewer 1, the accuracy of Reviewer 2 in detecting DMI was similar for each sequence, which may be attributed to the reviewer's extensive experience and high confidence. Previous studies have confirmed that empirical knowledge can improve the accuracy of DMI (30,31).

In our study, the accuracy of identifying DMI in both groups improved markedly with T1CE and mpMRI, and T1CE provided better contrast for detecting DMI (*Figure 1*). These findings highlight the significance of the information provided by T1CE and the necessity of combining multiple sequences for thorough interpretation. The findings of our study differ from those of Bhosale *et al.* (32). This could be because DWI had a large field of view in our investigation, resulting in low resolution. MpMRI had good diagnostic efficacy for the identification of DMI in both group A and B. However, compared with previous studies (33,34), our results showed a low sensitivity (60.0%, 3/5) and high specificity (96.9%, 63/65) for detecting DMI in group A. This was due to the fact that patients with EC-A have less DMI. A large sample study (17) from China showed that 50.14% (1,043/2,080) of patients with endometrial endometrioid carcinoma (EEC) without adenomyosis had SMI, whereas the incidence of SMI in patients with EEC with coexisting adenomyosis was 86.5% (199/230). Therefore, the sensitivity in group A to detect DMI was lower. This is also supported in the results of Erkilinç *et al.* (35), who noted that most cases of EC with coexisting adenomyosis were FIGO stage IA. The final sensitivity and specificity for our control group were similar to those in previous studies (9,36,37). Overall, the accuracy was similar to that in previous studies regardless of the presence of adenomyosis (38).

Although we consecutively collected 70 patients with EC-A, there were only 5 patients with DMI and this is an unavoidable limitation. The chi-square test showed that

2 out of 5 DMI cases were underestimated in group A, whrease only 4 out of 30 DMI cases were underestimated in group B. The results showed that there was no significant difference in detecting DMI (P=0.20). However, it is necessary to expand the sample size to further verify the impact of adenomyosis on the interpretation of MI depth in EC. Notably, although there was no significant difference in the accuracy of MRI for detecting DMI in patients with EC-A, the results showed higher AUC values in group B than those in group A for T2WI, DWI, and T1CE. Additionally, comparing the same sequence, the consistency of group B was higher than that of group A. These findings suggested that the presence of adenomyosis may reduce the diagnostic performance of the interpretation of MI in EC. A study by Haldorsen *et al.* (39) indicated that the overall agreement of radiologists in detecting DMI was fair [κ=0.39 (range, 0.26–0.55)]. In contrast, our study showed fair and good agreement with mpMRI in both the case and control groups (κ=0.387 *vs.* κ=0.695, respectively).

Our study showed that in 2 of the 70 cases of EC-A, the adenomyosis was not visible. A recent study by Bourdon *et al.* (40) confirmed that some adenomyosis lesions cannot be visualized on imaging. To further investigate the influence of adenomyosis subtype on the depth of MI, we classified adenomyosis on MRI into 4 subtypes. Overall, the different subtypes had no significant effect on the accuracy of detecting DMI. For Reviewer 1, focal adenomyosis and an affected size of <1/3 of the uterine wall had a higher misjudgment rate on T2WI. A plausible explanation is that there was a large difference in the sample sizes for these 2 subtypes. Therefore, a larger sample size is needed to explore the true effect of adenomyosis subtype on the depth of MI. Additionally, diagnosing DMI with T1CE in EC coexisting with external adenomyosis is significantly less accurate compared with internal adenomyosis. It is not surprising that T1CE increases the signal contrast between adenomyosis and EC, resulting in significantly higher accuracy for EC coexisting with internal adenomyosis.

Our study has the following limitations. First, all of the cancers were endometroid carcinomas and the small sample size especially regarding DMI cases due to objective reasons of prevalence. Second, this was a retrospective study, which may have led to selection bias. Third, factors such as MRI field strength or acquisition parameters with machines from different manufacturers may have increased the variability of the data between the 2 institutions participating in this study. However, we noticed that previous studies (29,41) also reported that images were acquired using several different MR machines, which is an accurate reflection of clinical practice; radiologists must read images acquired by different machines. Finally, the sample size used for performing MRI classification of adenomyosis was small and differed greatly.

Conclusions

The presence of adenomyosis may reduce the diagnostic performance of the interpretation of MI in EC. However, there was no significant difference in the accuracy of detecting DMI between the EC with coexisting adenomyosis and EC without adenomyosis groups, and between the different subtypes of adenomyosis. T1CE can increase the contrast between adenomyosis and cancer foci; therefore, the information provided by T1CE should be valued.

Acknowledgments

We thank Xinguang Zhao from Fushun Central Hospital and Zengyan Li from Shenzhen Luohu People's Hospital for their assistance in collecting the data and we thank Jane Charbonneau, DVM, from Liwen Bianji (Edanz) (www.liwenbianji.cn) for editing the English text of a draft of this manuscript.

Funding: This work was supported by the Beijing Hospitals Authority Clinical Medicine Development of Special Funding Support (No. ZYLX202101, to Z.Y.).

Footnote

Reporting Checklist: The authors have completed the STARD reporting checklist. Available at https://qims.amegroups.com/article/view/10.21037/qims-23-1621/rc

Conflicts of Interest: All authors have completed the ICMJE uniform disclosure form (available at https://qims.amegroups.com/article/view/10.21037/qims-23-1621/coif). The authors have no conflicts of interest to declare.

Ethical Statement: The authors are accountable for all aspects of the work in ensuring that questions related to the accuracy or integrity of any part of the work are appropriately investigated and resolved. The study was conducted in accordance with the Declaration of Helsinki (as revised in 2013). The study was approved by institutional ethics boards of Beijing Friendship Hospital Affiliated to

Capital Medical University (No. YYXSSC-2022-073) and Beijing Obstetrics and Gynecology Hospital Affiliated to Capital Medical University (No. 2022-KY-061-01). The requirement for individual consent for this analysis was waived due to the retrospective nature.

References

1. Siegel RL, Miller KD, Fuchs HE, Jemal A. Cancer Statistics, 2021. CA Cancer J Clin 2021;71:7-33.
2. Lin Z, Wang T, Li H, Xiao M, Ma X, Gu Y, Qiang J. Magnetic resonance-based radiomics nomogram for predicting microsatellite instability status in endometrial cancer. Quant Imaging Med Surg 2023;13:108-20.
3. Wang H, Xu Z, Zhang H, Huang J, Peng H, Zhang Y, Liang C, Zhao K, Liu Z. The value of magnetic resonance imaging-based tumor shape features for assessing microsatellite instability status in endometrial cancer. Quant Imaging Med Surg 2022;12:4402-13.
4. Sala E, Rockall A, Kubik-Huch RA. Advances in magnetic resonance imaging of endometrial cancer. Eur Radiol 2011;21:468-73.
5. Di Donato V, Giannini A, Bogani G. Recent Advances in Endometrial Cancer Management. J Clin Med 2023;12:2241.
6. Concin N, Matias-Guiu X, Vergote I, Cibula D, Mirza MR, Marnitz S, et al. ESGO/ESTRO/ESP guidelines for the management of patients with endometrial carcinoma. Int J Gynecol Cancer 2021;31:12-39.
7. Palmér M, Åkesson Å, Marcickiewicz J, Blank E, Hogström L, Torle M, Mateoiu C, Dahm-Kähler P, Leonhardt H. Accuracy of transvaginal ultrasound versus MRI in the PreOperative Diagnostics of low-grade Endometrial Cancer (PODEC) study: a prospective multicentre study. Clin Radiol 2023;78:70-9.
8. Maheshwari E, Nougaret S, Stein EB, Rauch GM, Hwang KP, Stafford RJ, Klopp AH, Soliman PT, Maturen KE, Rockall AG, Lee SI, Sadowski EA, Venkatesan AM. Update on MRI in Evaluation and Treatment of Endometrial Cancer. Radiographics 2022;42:2112-30.
9. Wang LJ, Tseng YJ, Wee NK, Low JJH, Tan CH. Diffusion-weighted imaging versus dynamic contrast-enhanced imaging for pre-operative diagnosis of deep myometrial invasion in endometrial cancer: A meta-analysis. Clin Imaging 2021;80:36-42.
10. Alcázar JL, Gastón B, Navarro B, Salas R, Aranda J, Guerriero S. Transvaginal ultrasound versus magnetic resonance imaging for preoperative assessment of myometrial infiltration in patients with endometrial cancer: a systematic review and meta-analysis. J Gynecol Oncol 2017;28:e86.
11. Bi Q, Chen Y, Wu K, Wang J, Zhao Y, Wang B, Du J. The Diagnostic Value of MRI for Preoperative Staging in Patients with Endometrial Cancer: A Meta-Analysis. Acad Radiol 2020;27:960-8.
12. Lee YJ, Moon MH, Sung CK, Chun YK, Lee YH. MR assessment of myometrial invasion in women with endometrial cancer: discrepancy between T2-weighted imaging and contrast-enhanced T1-weighted imaging. Abdom Radiol (NY) 2016;41:127-35.
13. Rockall AG, Meroni R, Sohaib SA, Reynolds K, Alexander-Sefre F, Shepherd JH, Jacobs I, Reznek RH. Evaluation of endometrial carcinoma on magnetic resonance imaging. Int J Gynecol Cancer 2007;17:188-96.
14. Foti PV, Farina R, Coronella M, Ruggeri C, Palmucci S, Montana A, Milone P, Zarbo G, Caltabiano R, Lanzafame S, Politi G, Ettorre GC. Endometrial carcinoma: MR staging and causes of error. Radiol Med 2013;118:487-503.
15. Otero-García MM, Mesa-Álvarez A, Nikolic O, Blanco-Lobato P, Basta-Nikolic M, de Llano-Ortega RM, Paredes-Velázquez L, Nikolic N, Szewczyk-Bieda M. Role of MRI in staging and follow-up of endometrial and cervical cancer: pitfalls and mimickers. Insights Imaging 2019;10:19.
16. Khalifa MA, Atri M, Klein ME, Ghatak S, Murugan P. Adenomyosis As a Confounder to Accurate Endometrial Cancer Staging. Semin Ultrasound CT MR 2019;40:358-63.
17. Chao X, Wu M, Ma S, Tan X, Zhong S, Bi Y, Wu H, Lang J, Li L. The clinicopathological characteristics and survival outcomes of endometrial carcinoma coexisting with or arising in adenomyosis: A pilot study. Sci Rep 2020;10:5984.
18. Raffone A, Seracchioli R, Raimondo D, Maletta M, Travaglino A, Raimondo I, Giaquinto I, Orsini B, Insabato L, Pellicano M, Zullo F. Prevalence of adenomyosis in

endometrial cancer patients: a systematic review and meta-analysis. Arch Gynecol Obstet 2021;303:47-53.
19. Utsunomiya D, Notsute S, Hayashida Y, Lwakatare F, Katabuchi H, Okamura H, Awai K, Yamashita Y. Endometrial carcinoma in adenomyosis: assessment of myometrial invasion on T2-weighted spin-echo and gadolinium-enhanced T1-weighted images. AJR Am J Roentgenol 2004;182:399-404.
20. Sala E, Crawford R, Senior E, Shaw A, Simcock B, Vrotsou K, Palmer C, Rajan P, Joubert I, Lomas D. Added value of dynamic contrast-enhanced magnetic resonance imaging in predicting advanced stage disease in patients with endometrial carcinoma. Int J Gynecol Cancer 2009;19:141-6.
21. Habiba M, Benagiano G. Classifying Adenomyosis: Progress and Challenges. Int J Environ Res Public Health 2021;18:12386.
22. Kishi Y, Suginami H, Kuramori R, Yabuta M, Suginami R, Taniguchi F. Four subtypes of adenomyosis assessed by magnetic resonance imaging and their specification. Am J Obstet Gynecol 2012;207:114.e1-7.
23. Kobayashi H, Matsubara S. A Classification Proposal for Adenomyosis Based on Magnetic Resonance Imaging. Gynecol Obstet Invest 2020;85:118-26.
24. Munro MG. Classification and Reporting Systems for Adenomyosis. J Minim Invasive Gynecol 2020;27:296-308.
25. Van den Bosch T, de Bruijn AM, de Leeuw RA, Dueholm M, Exacoustos C, Valentin L, Bourne T, Timmerman D, Huirne JAF. Sonographic classification and reporting system for diagnosing adenomyosis. Ultrasound Obstet Gynecol 2019;53:576-82.
26. Pecorelli S. Revised FIGO staging for carcinoma of the vulva, cervix, and endometrium. Int J Gynaecol Obstet 2009;105:103-4.
27. Ali A, Black D, Soslow RA. Difficulties in assessing the depth of myometrial invasion in endometrial carcinoma. Int J Gynecol Pathol 2007;26:115-23.
28. Takeuchi M, Matsuzaki K, Harada M. Evaluating Myometrial Invasion in Endometrial Cancer: Comparison of Reduced Field-of-view Diffusion-weighted Imaging and Dynamic Contrast-enhanced MR Imaging. Magn Reson Med Sci 2018;17:28-34.
29. Takeuchi M, Matsuzaki K, Nishitani H. Diffusion-weighted magnetic resonance imaging of endometrial cancer: differentiation from benign endometrial lesions and preoperative assessment of myometrial invasion. Acta Radiol 2009;50:947-53.
30. Woo S, Kim SY, Cho JY, Kim SH. Assessment of deep myometrial invasion of endometrial cancer on MRI: added value of second-opinion interpretations by radiologists subspecialized in gynaecologic oncology. Eur Radiol 2017;27:1877-82.
31. Saba L, Guerriero S, Sulis R, Pilloni M, Ajossa S, Melis G, Mallarini G. Learning curve in the detection of ovarian and deep endometriosis by using Magnetic Resonance: comparison with surgical results. Eur J Radiol 2011;79:237-44.
32. Bhosale P, Ma J, Iyer R, Ramalingam P, Wei W, Soliman P, Frumovitz M, Kundra V. Feasibility of a reduced field-of-view diffusion-weighted (rFOV) sequence in assessment of myometrial invasion in patients with clinical FIGO stage I endometrial cancer. J Magn Reson Imaging 2016;43:316-24.
33. Thieme SF, Collettini F, Sehouli J, Biocca L, Lella A, Wagner M, Almuheimid J, Plett H, Muallem MZ. Preoperative Evaluation of Myometrial Invasion in Endometrial Carcinoma: Prospective Intra-individual Comparison of Magnetic Resonance Volumetry, Diffusion-weighted and Dynamic Contrast-enhanced Magnetic Resonance Imaging. Anticancer Res 2018;38:4813-7.
34. Seo JM, Kim CK, Choi D, Kwan Park B. Endometrial cancer: utility of diffusion-weighted magnetic resonance imaging with background body signal suppression at 3T. J Magn Reson Imaging 2013;37:1151-9.
35. Erkilinç S, Taylan E, Gülseren V, Erkilinç G, Karadeniz T, Bağci M, Temel O, Solmaz U, Gökçü M, Sanci M. The Effect of Adenomyosis in Myometrial Invasion and Overall Survival in Endometrial Cancer. Int J Gynecol Cancer 2018;28:145-51.
36. Andreano A, Rechichi G, Rebora P, Sironi S, Valsecchi MG, Galimberti S. MR diffusion imaging for preoperative staging of myometrial invasion in patients with endometrial cancer: a systematic review and meta-analysis. Eur Radiol 2014;24:1327-38.
37. Deng L, Wang QP, Chen X, Duan XY, Wang W, Guo YM. The Combination of Diffusion- and T2-Weighted Imaging in Predicting Deep Myometrial Invasion of Endometrial Cancer: A Systematic Review and Meta-Analysis. J Comput Assist Tomogr 2015;39:661-73.
38. Lefebvre TL, Ueno Y, Dohan A, Chatterjee A, Vallières M, Winter-Reinhold E, Saif S, Levesque IR, Zeng XZ, Forghani R, Seuntjens J, Soyer P, Savadjiev P, Reinhold C. Development and Validation of Multiparametric MRI-based Radiomics Models for Preoperative Risk Stratification of Endometrial Cancer. Radiology 2022;305:375-86.

39. Haldorsen IS, Husby JA, Werner HM, Magnussen IJ, Rørvik J, Helland H, Trovik J, Salvesen ØO, Espeland A, Salvesen HB. Standard 1.5-T MRI of endometrial carcinomas: modest agreement between radiologists. Eur Radiol 2012;22:1601-11.
40. Bourdon M, Oliveira J, Marcellin L, Santulli P, Bordonne C, Maitrot Mantelet L, Millischer AE, Plu Bureau G, Chapron C. Adenomyosis of the inner and outer myometrium are associated with different clinical profiles. Hum Reprod 2021;36:349-57.
41. Stanzione A, Maurea S, Danzi R, Cuocolo R, Galatola R, Romeo V, Raffone A, Travaglino A, Di Spiezio Sardo A, Insabato L, Pace L, Scaglione M, Brunetti A, Mainenti PP. MRI to assess deep myometrial invasion in patients with endometrial cancer:A multi-reader study to evaluate the diagnostic role of different sequences. Eur J Radiol 2021;138:109629.

Cite this article as: Meng X, Liu M, Yang D, Jin H, Liu Y, Xu H, Liang Y, Wang Z, Wang L, Yang Z. Multiparametric magnetic resonance imaging-based assessment of the effect of adenomyosis on determining the depth of myometrial invasion in endometrial cancer. Quant Imaging Med Surg 2024;14(5):3717-3730. doi: 10.21037/qims-23-1621

Supplementary

Table S1 The MRI protocol parameters for GE (Signa Excite 1.5T)

Parameters	T1WI	T2WI			Contrast-enhanced T1WI			SS-EPI DWI
	Axial	Axial	Sagittal	Coronal	Axial	Sagittal	Coronal	Axial
Slice thickness, mm	4	4	4	4	4	4	4	4
Slice gap, mm	1.0	1.0	0.5	1.0	Volume scanning	Volume scanning	Volume scanning	1
TR, ms	400	2,700	3,000	3,000	3.6	4.1	4	4,000
TE, ms	8	68	102	85	1.7	5.1	1.9	74
Matrix	288×192	320×224	320×288	288×192	256×224	288×192	288×192	128×128
FOV, mm	320×320	300×300	260×260	40×400	360×360	320×320	360×360	360×360
b value, s/mm^2	–	–	–	–	–	–	–	0, 800
Average	2	4	2	4	2	2	2	4

MRI, magnetic resonance imaging; T1WI, T1-weighted imaging; T2WI, T2-weighted imaging; SS-EPI, single-shot echo-planar imaging; DWI, diffusion-weighted imaging; TR, repetition time; TE, echo time; FOV, field of view.

Table S2 The MRI protocol parameters for PHILIPS (3.0T Ingenia)

Parameters	T1WI	T2WI			Contrast-enhanced T1WI			SS-EPI DWI
	Axial	Axial	Sagittal	Coronal	Axial	Sagittal	Coronal	Axial
Slice thickness, mm	4	4	4	4	4	3	4	4
Slice gap, mm	-2	1	1	1	–2	–1.5	–2	1
TR, ms	4.0	4,009	3,546	4,418	3.8	3.6	3.5	6,000
TE, ms	1.44	100	98	80	1.33	1.32	1.3	53
Matrix	316×235	320×320	316×316	400×312	268×220	240×198	252×221	120×93
FOV, mm	380×304	240×240	253×253	280×280	400×353	360×320	400×353	300×238
b value, s/mm^2	–	–	–	–	–	–	–	0, 1,000
Average	1	1.3	1	1.2	1	1	1	3

MRI, magnetic resonance imaging; T1WI, T1-weighted imaging; T2WI, T2-weighted imaging; SS-EPI, single-shot echo-planar imaging; DWI, diffusion-weighted imaging; TR, repetition time; TE, echo time; FOV, field of view.

https://dx.doi.org/10.21037/qims-23-1621

Table S3 The MRI protocol parameters for Siemens (Prisma 3.0T)

Parameters	T1WI	T2WI			Contrast-enhanced T1WI			Resolve DWI
	Axial	Axial	Sagittal	Coronal	Axial	Sagittal	Coronal	Axial
Slice thickness, mm	3	4	4	4	2	2.5	3	4
Slice gap, mm	0.6	0.8	1.2	0.8	0.1	0.5	0.6	0.8
TR, ms	4.02	3,800	4,800	7,000	4.54	3.14	3.16	4,100
TE, ms	1.32	83	116	74	2.1	1.17	1.11	50
Matrix	188×320	240×320	288×384	210×320	195×320	175×320	182×320	72×128
FOV, mm	360×281	240×240	230×230	280×245	320×260	350×273	380×310	360×200
b value, s/mm^2	–	–	–	–	–	–	–	0, 1,000
Average	1	1	1	1	1	1	1	3

MRI, magnetic resonance imaging; T1WI, T1-weighted imaging; T2WI, T2-weighted imaging; DWI, diffusion-weighted imaging; TR, repetition time; TE, echo time; FOV, field of view.

Table S4 The MRI protocol parameters for GE (750W 3.0T)

Parameters	T1WI	T2WI			Contrast-enhanced T1WI			SS-EPI DWI
	Axial	Axial	Sagittal	Coronal	Axial	Sagittal	Coronal	Axial
Slice thickness, mm	5.5	4	4	4	3.0	2	3	5.5
Slice gap, mm	1.0	1.0	0.5	0.5	Volume scanning	Volume scanning	Volume scanning	1
TR, ms	600	5,725	3,860	4,451	4.5	4.3	4.0	4,245
TE, ms	42	85	102	102	1.7	2	2.4	80
Matrix	320×224	300×256	384×256	320×256	288×224	288×192	256×224	128×128
FOV, mm	300×300	300×300	280×280	280×280	360×360	340×340	480×480	320×320
B value, s/mm^2	–	–	–	–	–	–	–	0, 1,000
Average	2	4	4	2	2	2	1	4

MRI, magnetic resonance imaging; T1WI, T1-weighted imaging; T2WI, T2-weighted imaging; SS-EPI, single-shot echo-planar imaging; DWI, diffusion-weighted imaging; TR, repetition time; TE, echo time; FOV, field of view.

https://dx.doi.org/10.21037/qims-23-1621

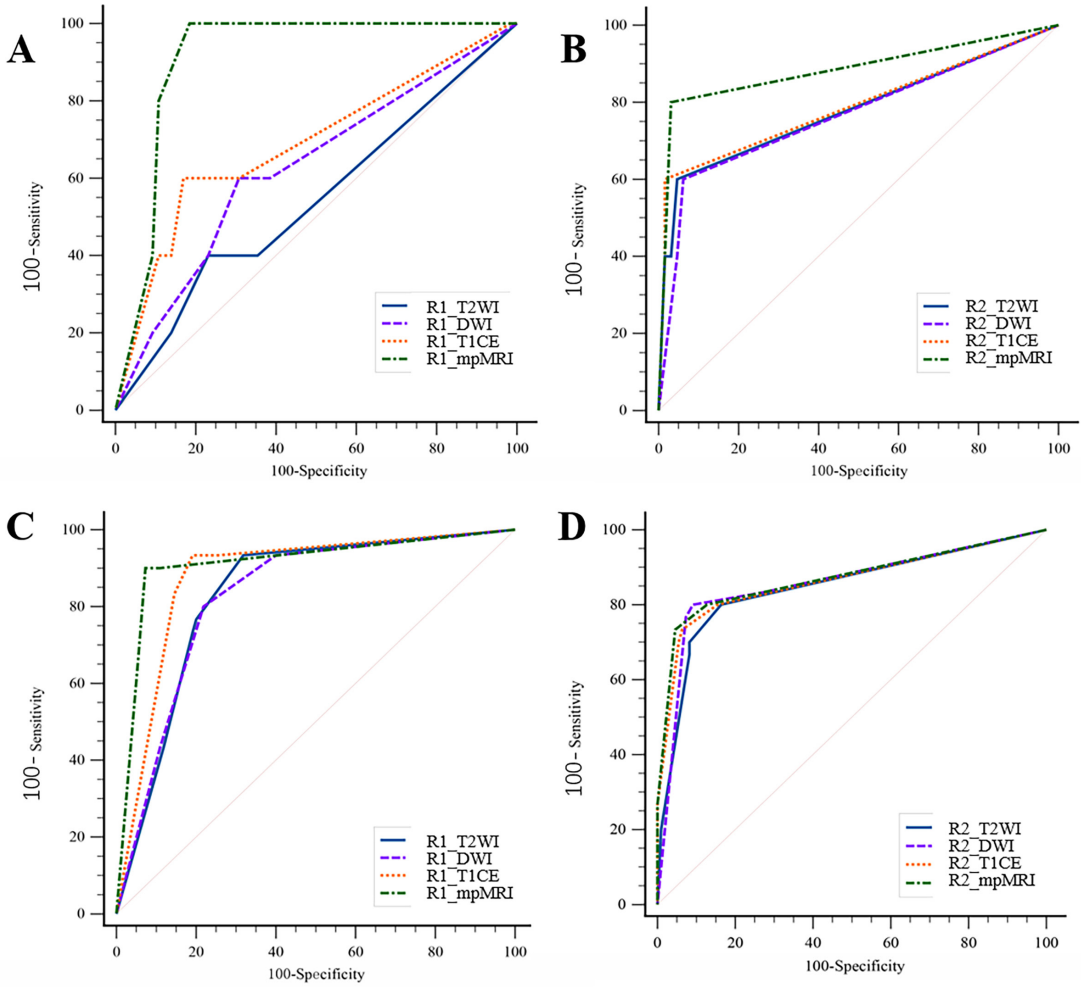

Figure S1 The AUROC for identifying DMI. The 4 curves represent the diagnostic performance of T2WI, DWI, DCE, mpMRI, respectively. (A-D) represent the AUROC of reviewer 1 in group A, reviewer 2 in group A, reviewer 1 in group B and reviewer 2 in group B, respectively. Group A, patients with endometrial cancer coexisting with adenomyosis; Group B, patients with endometrial cancer without coexisting with adenomyosis. R1, reviewer 1; R2, reviewer 2; T2WI, T2-weighted imaging; DWI, diffusion-weighted imaging; T1CE, T1-weighted contrast-enhanced; mpMRI, multiparametric magnetic resonance imaging; DMI, deep myometrial invasion; AUROC, area under the receiver operating curve.

https://dx.doi.org/10.21037/qims-23-1621

Table S5 Interpretation results of two reviewers and consensus for different subtypes of adenomyosis on T2WI, DWI, T1CE, mpMRI

Reviewer	Sequence	Status	Spatial relationship			Affected area			Affected pattern			Affected size			
		Correct interpretation	Adjacent	Non-adjacent	P value	Internal adenomyosis	External adenomyosis	P value	Diffuse	Focal	P value	<1/3 of uterine wall	<2/3 of uterine wall	>2/3 of uterine wall	P value
R1	T2WI	Yes	18	30	0.184	42	6	0.279	37	11	0.028*	6	15	27	0.045*
		No	11	9		15	5		10	10		6	9	5	
	DWI	Yes	19	30	0.300	43	6	0.269	36	13	0.212	8	14	27	0.081
		No	10	9		14	5		11	8		4	10	5	
	T1CE	Yes	24	33	1.000	51	6	0.012*	42	15	0.082	9	19	29	0.340
		No	5	6		6	5		5	6		3	5	3	
	mpMRI	Yes	24	36	0.272	52	8	0.113	43	17	0.240	11	19	30	0.255
		No	5	3		5	3		4	4		1	5	2	
R2	T2WI	Yes	27	36	1.000	54	9	0.181	45	18	0.167	10	23	30	0.395
		No	2	3		3	2		2	3		2	1	2	
	DWI	Yes	27	36	1.000	53	10	1.000	45	18	0.167	11	22	30	1.000
		No	2	3		4	1		2	3		1	2	2	
	T1CE	Yes	28	36	0.631	55	9	0.120	46	18	0.084	10	24	30	0.121
		No	1	3		2	2		1	3		2	0	2	
	mpMRI	Yes	28	36	0.631	55	9	0.120	46	18	0.084	10	24	30	0.121
		No	1	3		2	2		1	3		2	0	2	
Consensus	mpMRI	Yes	27	37	1.000	54	10	0.515	45	19	0.582	11	23	30	1.000
		No	2	2		3	1		2	2		1	1	2	

*, P<0.05. T2WI, T2-weighted imaging; DWI, diffusion-weighted imaging; T1CE, T1-weighted contrast-enhanced imaging; mpMRI, multiparametric magnetic resonance imaging; R1, reviewer 1; R2, reviewer 2.

https://dx.doi.org/10.21037/qims-23-1621